Hindawi Publishing Corporation
Journal of Nanomaterials
Volume 2011, Article ID 527437, 10 pages
doi:10.1155/2011/527437

Research Article

Application of Flow Focusing to the Break-Up of a Magnetite Suspension Jet for the Production of Paramagnetic Microparticles

Lucía Martín-Banderas,[1,2] Román González-Prieto,[3] Alfonso Rodríguez-Gil,[4] Mercedes Fernández-Arévalo,[1] María Flores-Mosquera,[2] Sebastián Chávez,[4] and Alfonso M. Gañán-Calvo[2,5]

[1] *Department of Pharmacy and Pharmaceutical Technology, Faculty of Pharmacy, University of Seville, 41012 Seville, Spain*
[2] *R&D Department, Ingeniatrics Tecnologías S.L., 41900 Camas (Seville), Spain*
[3] *Centro Andaluz de Biología Molecular y Medicina Regenerativa, CABIMER-CSIC, 41092 Seville, Spain*
[4] *Department of Genetics, Faculty of Biology, University of Seville, 41012 Seville, Spain*
[5] *Department of Aerospace Engineering and Fluids Mechanics, ESI, University of Seville, 41092 Seville, Spain*

Correspondence should be addressed to Alfonso M. Gañán-Calvo, amgc@us.es

Received 31 May 2010; Accepted 25 July 2010

Academic Editor: Lu Sun

Copyright © 2011 Lucía Martín-Banderas et al. This is an open access article distributed under the Creative Commons Attribution License, which permits unrestricted use, distribution, and reproduction in any medium, provided the original work is properly cited.

Paramagnetic particles offer an extensive improvement in the magnetic separation or purification of a wide variety of protein molecules. Most commercial paramagnetic particles are synthesized by laborious and costly procedures. A straightforward production of paramagnetic microparticles with homogeneous and selectable sizes using flow focusing (FF) technology is described in this work. The development of an initial formulation of a stable iron oxide suspension compatible with the FF requirements is also reported. The obtained particles, below 10 microns in diameter and presenting smooth and reactive surface, were codified with an organic fluorophore and showed excellent properties for covalent attachment of biomolecules such as proteins and its subsequent recognition by flow cytometry. Furthermore, particles with suitable magnetite content resulted as well-suited for commercial magnet separators for these purposes.

1. Introduction

Magnetic polymer particles usually consist of a core of silica or polystyrene covered by paramagnetic nanoparticles, typically iron oxide. In other cases iron oxide is entrapped within a polymer matrix that can be engineered to exhibit the desired physical and chemical properties, providing a reactive surface to which proteins and polynucleotides can be conjugated. The conventional methods for preparing paramagnetic microparticles include (a) swelling [1], (b) dispersion polymerization [2], (c) emulsion polymerization [3], (d) emulsion-solvent extraction-evaporation [4], (e) porous membranes [5], (f) layer-by-layer [6], (g) conventional sol-gel method [7].

Commercial particles for these purposes are produced by a multiple-step procedure resulting in a laborious and costly production process.

Magnetic particles offer high potential benefits in multiple fields, particularly in biotechnology and biomedicine. According to their use in these later fields, they can be simply classified into two wide groups: particles for *in vivo* or *in vitro* [8–10] applications. In biochemical applications, the use of these particles for multiplexed assays constituted a particularly useful tool, allowing homogeneous results, facilitating the sample manipulation, and avoiding the risk of sample loss.

In these uses, paramagnetic microparticles need to satisfy the following prerequisites: they should be stable in water, uniform in size, and responsive to magnetic field gradients. In addition, they must be identifiable by a suitable system (usually by an optical codification system) [10–16].

Here we report a very versatile and controlled procedure for the production of dye-labelled solid paramagnetic polymeric microparticles, yielding remarkable size accuracy with

negligible size dispersion and allowing surface engineering or design. We demonstrate some crucial advantages over alternative methods for the size ranges considered in this work (from about 1 to 10 microns):

(i) high production rate from a single nozzle (some orders of magnitude by multiplexing can be scaled up though this is out of the scope of present work),

(ii) one-step production,

(iii) selectable size using the same device,

(iv) strict control on the particle size distribution (zero-rejection production).

The first stage of the synthesis procedure implies the elaboration of a stable magnetite suspension. We have evaluated several stabilizing agents to obtain a suitable magnetite suspension compatible with a standard Flow Focusing (FF) nozzle. Then, we directly utilize the magnetite suspension to produce nearly monodisperse drops without any external excitation source or additional purification steps [17] inside a continuous phase. Those drops yield solid microspheres through solvent extraction by the continuous phase. This approach allows the production of magnetic fluorescent-encoded beads with a uniform morphology, narrow diameter distribution, and controlled and suitable fluorescent and magnetic properties in a one-step easy way. Magnetic properties were evaluated by a simple magnetic separation test and by measuring magnetite content. The effectiveness of the microbead array for covalent attachment of biomolecules was tested in a quantitative way. Finally, the ability of the fluorescently labeled microspheres for the detection of biomolecule interactions using flow cytometry was also tested, extending the study of previously synthesized "barcoded" particles produced by the FF technology [18].

1.1. Flow Focusing Technology. In short, FF is a simple and low-cost atomization technique based on the combination of a specific geometry and hydrodynamic forces providing a remarkable accuracy in size, narrow size dispersion, and feasibility. The appropriate fluid combinations allow not only particles to be obtained but also monodisperse bubbles, sprays, or emulsions at micro- and nanoscales. The phenomenon is characterized by the presence of a steady microjet which is "sucked" through a small orifice and eventually breaks up into droplets of well-defined size under very gentle operation conditions and reliability [19].

One of its most important innovative applications is the possibility of obtaining solid microparticles by means of solidifying the controlled-size microdrops generated. Depending on the nature of the fluids employed, different solidifying processes can be used: thermal solvent evaporation/extraction, cooling of melted materials, chemical hardening, UV-curable monomers, and so forth. As the drops are generated with a precise, narrow size distribution, the solid particles maintain the same geometrical features. In addition, this technology is suitable for particle engineering through the manipulation of its internal morphology, all in one-step: depending on the use of single, multiple or coaxial feeding capillaries, homogeneous particles, or single/multivesicle microcapsules with one or multiple shells of controllable thickness can be achieved. Some nice examples of particle production by FF technology are controlled multicore microcapsules [20], poly(lactic-co-glycolic acid) (PLGA) particles for drug encapsulation of hydrophilic (gentamicin sulphate) [21] and lipophylic (lidocaine) drugs and also for proteins such us green fluorescent protein [22, 23], solid lipid particles obtained by spray cooling using a special thermostated FF nozzle [21], or encoded fluorescent microparticles for biomolecules detection [17, 18].

One of the main advantages of FF technology is the predictability of the final microparticle diameter with a remarkable accuracy. In the present work, the FF technology was adapted to the solvent extraction encapsulation method using a simple FF liquid-liquid configuration. In this case, the drop diameter (d_g) could be calculated from the expression of the jet diameter (d_j) as

$$d_g = \left(\frac{3\pi}{2k}\right)^{1/3} d_j, \tag{1}$$

where k is the wavenumber of the fastest growing perturbation on the jet (approximately $k \approx 0.5$ for most liquid-liquid combinations) which depends on the viscosities and densities ratios between the inner and outer liquids [20, 24]. The jet diameter depends on geometry of the nozzle (mainly D, orifice diameter) and the operating conditions (mainly the liquid flow rates; see references [18, 25, 26]) only. Hence, the final droplet diameter can be written as

$$d_g = \left(\frac{3\pi}{2k}\right)^{1/3} \left(\frac{Q_d}{Q_t}\right)^{1/2} D, \tag{2}$$

where Q_d and Q_t are the inner and outer fluid flow rates, respectively.

The particle diameter (d_p) is calculated by taking into account the drop diameter, the polymer density (ρ_p), and the polymer concentration (C, mass of polymer per volume of solution):

$$d_p = \left(\frac{3\pi C}{2k\rho_p}\right)^{1/3} \left(\frac{Q_d}{Q_t}\right)^{1/2} D. \tag{3}$$

Thus, given a desired final particle diameter, it is possible to set up the experimental conditions so as to drastically reduce the numbers of trials, or, conversely, for a specific flow rate combination and properties of the liquids, the final particle diameter can be predicted.

Several technological approaches have been previously used to synthesize magnetic particles for these purposes. However, important limitations were found related to

(i) the nozzle geometry, where even the nozzle orientation affected the particle morphology due to the effect of gravity forces [27],

(ii) the nozzle fabrication: nozzles fabricated in PMDS (poly(dimethylsiloxane)) by soft lithography needed to be pretreated to avoid wetting problems and presented leak problems [27–29],

(iii) the method applied for drop solidification such us UV-curable monomers, which required the application of high temperatures for long times (60°C, overnight) [28] and to remove monomer in excess [29] or to employ toxic reactants such us glutaraldehyde as a cross-linker agent [30].

2. Materials and Methods

2.1. Materials. The following chemicals were purchased from Sigma-Aldrich (USA) and were used as received: polystyrene (PS) (M_w = 4000–200000); poly(styrene-co-maleic acid) partial isobutyl/methyl ester (PSMiso); poly(styrene-co-maleic acid) partial sec-butyl/methyl esther (PSMsec); rhodamine B; magnetite Fe_3O_4 98%, dichloromethane (DCM) 99.9% grade HPLC; oleic acid; polyvinyl alcohol (PVA), MW 72000; protein G, protein A, and fluorescein-labelled rabbit antimouse antibody. Ethyl acetate (EA) PRS was obtained from *Panreac Química S.A.* (Barcelona, Spain), Ethocel from The Dow Chemical Company, and Aerosil 200 Pharma, Eudragit RS PO, and Eudragit S100 from *Degussa AG*, Barcelona, Spain.

2.2. Methods

2.2.1. Preparation of Magnetite Suspension. To elaborate the paramagnetic nanoparticle suspension, oleic acid, silicon oxide (Aerosil 200 Pharma), cellulose (Ethocel), and methacrylates (Eudragit RS PO, Eudragit S100) were assayed as stabilizing agents.

As a carrier, a 4% w/v polymer solution was prepared in ethyl acetate (EA). Then, the stabilizing agent was codissolved or dispersed in that solution at different concentrations (0.6–1.5% w/v). After this, an accurately weighed aliquot of the paramagnetic nanomaterial (40–160 mg), 20–30 nm in size, was added and dispersed by sonication for 5 minutes. The newly prepared suspension was left standstill for 60 minutes. To evaluate the degree of sedimentation, several images of the suspension in a 10 mL glass vial were taken at 0, 10, 30, and 60 minutes. Finally, the presumed stable suspension was filtered through a 15–20 μm filter (Albet LabScience, Spain).

2.2.2. Preparation of Paramagnetic Microparticles by FF. An axisymmetric FF device was employed to prepare the paramagnetic microparticles at 25 ± 1°C in a simple liquid-liquid configuration, adapting the technology to the traditional emulsion-evaporation/extraction microencapsulation method (see Figure 1(a)).

A simple FF nozzle, model Avant (with geometric dimensions D = 100 μm, D_0 = 150 μm, and H = 100 μm; see Figure 1(a)) (Ingeniatrics Tecnologías S.L., Spain) was used to produce an o/w emulsion (see Figure 1(b)). The magnetite suspension, oil phase (focused fluid), was injected using a syringe pump (Harvard Apparatus, mod. "44" programmable, 55–1144) rated at 0.25–2 mL/h. The aqueous phase, distilled water (focusing fluid) was injected through

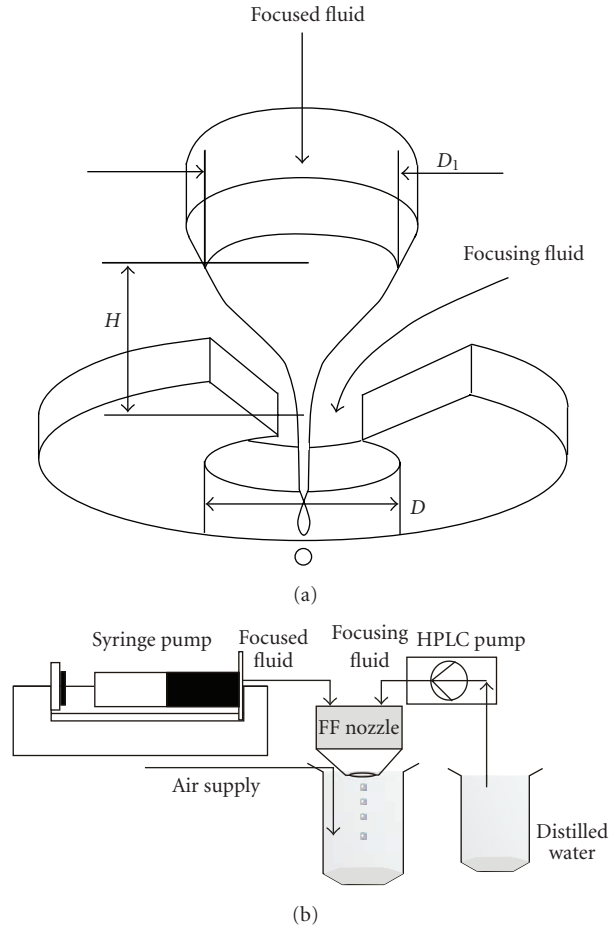

Figure 1: A simple FF nozzle (a) Scheme of functioning (D1 inner diameter of capillary tube, H distance capillary tube and nozzle exit, D diameter of exit orifice); (b) Experimental setup for paramagnetic microparticle production adapting FF to the traditional microencapsulation method emulsion-evaporation of solvent.

an HPLC pump (Shimadzu Corp. mod. LC-10AD vp, Germany) at 2–4 mL/minute.

With a proper control of the relative flow rates of the two fluids employed, the oil phase steady microjet (magnetite suspension) issuing from the nozzle became unstable at a certain station and broke into uniform droplets [19, 25, 26]. To avoid microdrop coalescence or deformation, the emulsion was produced in a bath containing a PVA solution 1% w/v under agitation for 3 hours by continuous air bubbling. After this time, the solvent was evaporated and the microdrops formed solid microparticles which were collected by centrifugation (4500 rpm, 10 minutes, Orto Alresa, mod. Digicen, Spain) and washed three times with fresh distilled water. The microparticles were then stored either as dry powder after freeze-drying [frozen in liquid nitrogen and lyophilized at −80.0 ± 0.5°C and 0.057 mbar; (Telstar, Cryodos, Spain)] or as a suspension, in distilled water containing sodium azide (0.2% w/v) to avoid microbial growth, and stored at 4.0 ± 0.5°C , in order to increase

their physicochemical stability but without significantly modifying their characteristics.

To produce encoded paramagnetic microparticle with an optically identifiable code, rhodamine B was used as a model fluorophore. It was codissolved with the polymer in ethyl acetate at 0.2 mM concentration.

2.2.3. Characterisation of the Paramagnetic Microparticles (MPs). The shape and surface characteristics of the microspheres were determined by scanning electron microscopy (SEM) (Philips XL-30, USA) after coating lyophilised samples with a gold thin film. MP diameters of nonlyophilised samples were determined under conventional microscopy (Leica DM LS) using an image-processing program (Image J. 1.30 v). Diameters from 500–1000 microparticles randomly selected from various micrograph images were measured and statistically processed. Results obtained were confirmed by SEM.

The magnetite content was determined by measuring the content of Fe atoms in lyophilised samples by inductively coupled plasma mass spectrometry (ICP-MS) (Thermo Elemental X-7, Termo Scientific) at 259.940 nm. Samples were previously digested in a microwave digester (Anton Para, mod. 3000) by adding nitric acid and hydrogen peroxide.

The magnetite content was expressed as an encapsulation efficiency percentage (%EE):

$$\%\text{EE} = \left(\frac{Q}{Q_i}\right) * 100, \tag{4}$$

where Q is the amount of magnetite encapsulated and Q_i the initial magnetite amount employed.

The paramagnetic microparticle behaviour under covalent coupling protocol conditions was also studied. The effect of pH and temperature on microparticle aspect and morphology was evaluated for different periods of time.

2.2.4. Magnetic Separation Test. Magnetic particles 5 μm in diameter, dispersed in 50 mL distilled water at a concentration of $\approx 10^7$ particles/mL were placed in a commercial magnetic separator (Merck ref. 69964). After prefixed intervals of time, an aliquot from supernatant was evaluated by counting the number of free particles in suspension using a Bürker camera.

2.2.5. Coupling of Protein G/A and Interaction Detection. In order to evaluate the affinity binding capacity of synthesized particles protein coupling assays were performed by the carbodiimide method as in previous work [18]. This is the most extensively used approach for coupling biomolecules to carboxylated surfaces. The method consists of activating carboxylic acid groups towards amide or ester formation.

Briefly, for protein conjugation, particles were activated with a freshly 1-ethyl-3-(3-dimethylaminopropyl)carbodiimide (EDC) solution in an activating medium, MES pH 5.4, for 20 minutes under stirring at room temperature. After several centrifugal washings microparticles were resuspended in coupling buffer, PBS pH 7.4, containing protein A or G. Then, particles were incubated for 2 hours under stirring agitation. After this, particles were collected by centrifugation (13000 rpm, 2 minutes; Eppendorf) and washed three times with washing buffer, MES 50 mM, NaCl 2 M and Tween 20 0.02%, pH 6. Finally, a blocking solution was added, PBS, NaN_3 0.1%, and BSA 1%, pH 7.4.

Table 1: Formulations tested to produce paramagnetic microparticles by using a FF simple nozzle (for F3 to F9. C_{polym} indicate polymer mixes of PS + PSM).

Formulation	C_{polym} (%w/v)	Stabilizing agent(%w/v)			Magnetite (%w/v)
		Aerosil	Ethocel	Eudragit RSPO	
F1	1	0.6	—	—	0.4
F2	1	—	—	0.6	0.4
F3	0.5 + 0.5	0.6	—	—	0.4
F4	1.4 + 0.6	0.6	—	—	0.4
F5	1.4 + 0.6	0.9	—	—	0.4
F7	2.8 + 1.2	0.6	—	—	0.4
F8	2.8 + 1.2	1.8	—	—	0.4
F9	2.8 + 1.2	0.9	—	—	0.4
F11	4	1.8	—	—	0.4
E2	4	—	1	—	0.6
E3	4	—	1.5	—	0.8
E5	4	0.6	1	—	0.6

3. Results

3.1. Stability of Magnetite Suspension. As it was previously indicated, to produce the paramagnetic microparticles by a simple FF device, the formation of a paramagnetic nanomaterial suspension was required, constituting the focused fluid. This suspension had to be stable for the time necessary to guarantee the formation of particles with a minimal and homogeneous content in magnetite.

This was a crucial and difficult goal due to the density of magnetite, 4.8–5.1 g/L. The time required for a suspension to be considered stable was fixed at 60 minutes.

Different results were obtained depending on the material employed as stabilizing agent. The best results in terms of suspension stability were achieved with Aerosil 200 Pharma at concentrations over 12% w/w, which were capable of producing stable suspensions after 72 hours. The rest of the formulations were excluded for MP production due to suspension instability.

3.2. Microparticle Morphology and Aspect. The SEM images in Figure 2 are representative of the paramagnetic microparticle populations 5 μm in diameter prepared by FF. A TEM image of commercial magnetite is also included (Figure 2(i)) (Philips CM-10). The surface features of the microparticles depended on the stabilizing agent employed and its concentration.

As it can be seen, spherical microparticles were obtained in all cases with the exception of the particles prepared with Eudragit RS PO (Figure 2(b)). In those cases where

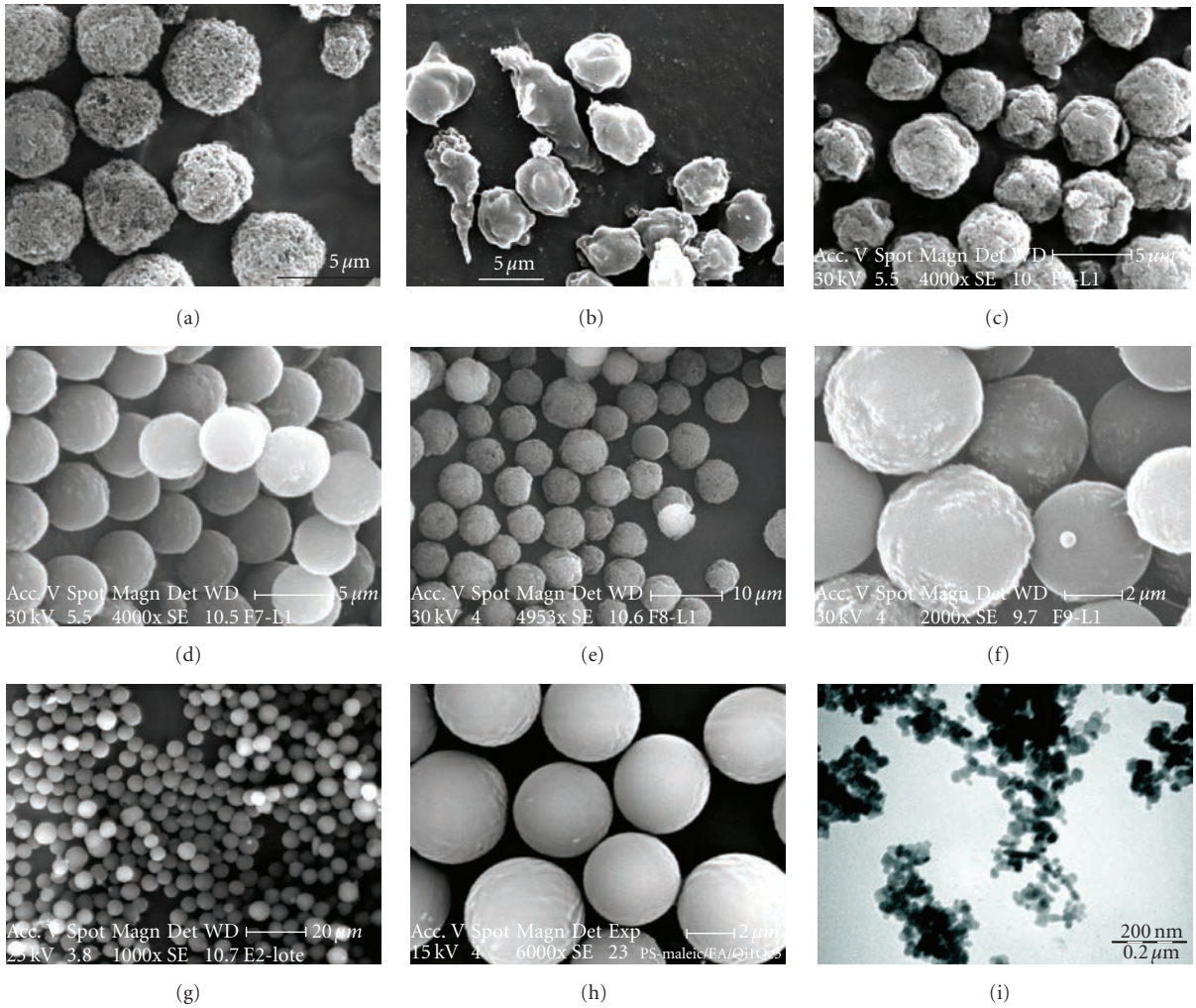

Figure 2: MPs aspect and morphology for formulations indicated: (a) F1; (b) F2, elaborated with Eudragit RSPO; (c) F5; (d) F7; (e) F8; (f) F9; (g) E3; (h) blank particles and, (i) TEM image of magnetite employed.

Aerosil or Ethocel was employed as stabilizing agents for the primary magnetite suspension, spherical particles were achieved although the particle surfaces depended on the magnetite/polymer/stabilizer ratio.

The effect of polymer concentration can be observed in Figures 2(a), 2(c), and 2(e). In these cases, the polymer concentration was 1, 2, and 4% w/v, respectively, and the stabilizing agent concentration was 30% w/w. Interestingly enough, as the polymer concentration increased, more regular spherically shaped particles were obtained. When the polymer concentration was kept at 4% w/w and the Aerosil concentration decreased from 30 to 12% w/w, it was possible to obtain particles with almost smooth surfaces (see Figures 2(d), 2(e), and 2(f)). This is an important aspect, because particles with highly porous surfaces promote unspecific unions that pose hindrances to the final application [31].

Ethocel, a water-insoluble ethyl cellulose used worldwide for many different functional purposes in pharmaceutical products, was also employed as a stabilizing agent in the range of 9 to 25% w/w. Figure 2(g) shows an example of this type of particle. In all cases, spherical smooth particles were obtained (similar pictures not shown were obtained for the rest of the formulations tested). For illustrative purposes, Figure 2(h) shows "blank" particles, without magnetite.

3.3. Microparticle Size and Size Distribution. In the experiments here reported, particle size analysis showed nearly monosized particles with selectable size between 3 and 10 μm in diameter, almost five times smaller than some published examples of magnetic particles obtained using devices based on FF principle [27–30].

Table 2 summarizes the diameters obtained as a function of polymer and Aerosil concentration using a flow rate of 3 mL/minute for the focusing fluid and 1 mL/hour for the focused fluid (magnetite suspension).

In order to determine the versatility of the particular FF device designed for the particle production, the possibility of producing paramagnetic microparticles with programmable or selectable sizes using the same nozzle was studied. For this purpose, several combinations of fluid rates were tested to

Table 2: MPs size as a function of polymer and Aerosil concentration (Magnetite 4% w/v, Qt 3 mL/min, Qd 1 mL/h).

Formulation	D th (μm)	D_{medium} (μm)	SD (μm)	VC (%)	GSD
F2	4.0	3.73	0.59	15.96	1.18
F3		3.80	0.39	10.34	1.10
F4	4.7	4.94	0.41	8.37	1.09
F5		4.95	0.49	9.86	1.09
F7	5.2	5.55	0.53	9.61	1.10
F8	6.2	6.03	0.67	11.06	1.12
F9	5.8	6.09	0.75	12.29	1.34
F11	5.8	5.78	0.25	4.39	1.05

obtain particles below 10 μm in diameter (some of them are shown in Figure 3). The formulation used for this study was F11. Figure 3 shows some of the results obtained.

For a given flow of focused fluid, an increase of the focusing liquid rate of flow leads to a decrease of the microparticle diameters. For a fixed focusing liquid rate of flow, an increase of the focused fluid flow rate leads to an increase in diameter(3). Thus, using a single nozzle with fixed geometrical parameters, it is possible to provide the required microparticle size by a simple adjustment of the liquid flow rates. The process setup also allowed the high-throughput synthesis of particles (10^9 particles per hour and per nozzle) in a continuous manner superior to related procedures for the production of magnetic particles described in the literature [27–29, 32].

The reproducibility of the process was also confirmed. Using flow rates Q_d = 1 mL/hour and Q_t = 3 mL/minute, the intralot diameter was 5.78 μm ± 0.25 μm with a VC equal to 4.39% ($n = 5$). The incorporation of rhodamine B into these polystyrene particles did not modify the final particle diameter.

In all cases, the experimental data were in accordance with the theoretical FF predictions (theoretical diameters are included in Figure 3). Successful results using the same mathematic model have been also reported for other loaded microparticles [21, 23].

3.4. Magnetite Content . The magnetite content was determined by ICP by measuring the Fe atom percentage. The theoretical Fe atom percentage in magnetite is 70.9%. Elemental analysis gave 69.2%. This experimental datum was used as the reference to calculate particle magnetite content.

Table 3 lists the results for the indicated formulations.

The best results were obtained using Aerosil as stabilizing agent, yielding an EE% of 74%. In the case of formulations with Ethocel, the maximum EE was about 28%. These results can be explained probably due to a more stable magnetite suspension obtained using Aerosil as stabilizing agent.

3.5. Microparticle Stability in Covalent Coupling Protocols. The aim of this brief study was to test the stability of microparticles under the pH, temperature, and time conditions involved in a covalent union process, following the usual protocols for *multiplex* assays.

Table 3: Magnetite content determined by ICP for formulations indicated (mean ± SD).

Sample	Fe_th (% w/w)	Fe_exp. (% w/w)	EE% (Fe)	EE% (magnetite)
Magnetite	70.91	69.784 ± 0.33	—	—
F8	4.48	3.09 ± 0.23	68.94 ± 0.30	74.01 ± 0.27
F9	4.48	0.605 ± 0.15	13.50 ± 0.53	14.49 ± 0.48
F11	4.48	2.382 ± 0.46	53.14 ± 0.45	57.05 ± 0.43
E2	6.84	1.22 ± 0.39	17.84 ± 0.49	19.15 ± 0.29
E3	7.53	1.80 ± 0.27	26.32 ± 0.38	28.26 ± 0.17
E5	6.73	1.22 ± 0.38	18.14 ± 0.60	19.47 ± 0.58

Table 4: Experimental conditions for paramagnetic microparticles stability study (particles were 5 μm in diameter).

Medium	pH	T (°C)	Time (h)	
PBS	7	37	2	4
MES	6	37	2	4
PBS-BSA	7.4	37	2	4
DENHART	8	90	10 minute	—
		55	2	4

Three types of polystyrene were employed as the polymer matrix formed to prepare the paramagnetic particles: PS, PSMiso, and PSMsec. Particles 5 μm in diameter were dispersed in different media and observed under optical microscopy at preset times (see Table 4).

In PBS (pH 7), MES (pH 6), and PBS-BSA (pH 7.4) media, the microparticles maintained their morphology and size at 37°C for 4 hours, independently of the polymeric matrix composition.

The particles prepared with PSMsec also kept their properties at 90°C for 10 minutes and 55°C in Denhart medium (pH 8) for 4 hours, in contrast to those elaborated employing PSMiso. In this case, the particles showed a clear halo, began to dissolve and swelled, increasing their size in the first minutes of the assay (see Figure 4).

In view of these results, PSMsec was selected as the optimal polymer to prepare the MPs. Like the PSMiso, this polymer presents carboxyl groups at a high density (acid value ~ 180 mg KOH/g) which facilitates covalent unions. The improved stability of PSMsec could be due to the chemical structure of the sec-butyl residue that precludes any reagent to approach the carboxyl group.

3.6. Magnetic Separation Test. Highly magnetic particles are particularly useful in an immunoassay for their faster separations and thus faster assays becoming possible. Results obtained from this test are nicely shown in Figure 5, where the magnetic separation of F11 and E3 particles suspensions was very similar, confirming the higher magnetization of both formulations.

3.7. Immunoassays. Selected paramagnetic microparticles obtained were evaluated for immunoprecipitation assays.

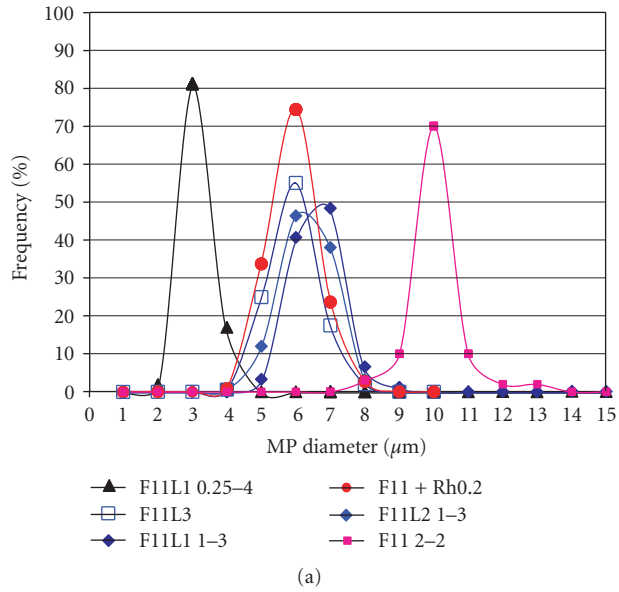

(a)

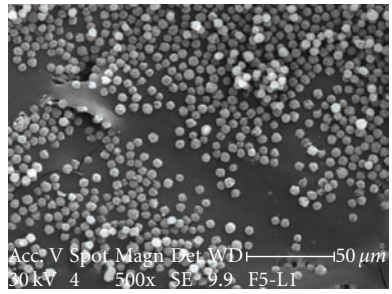

(b)

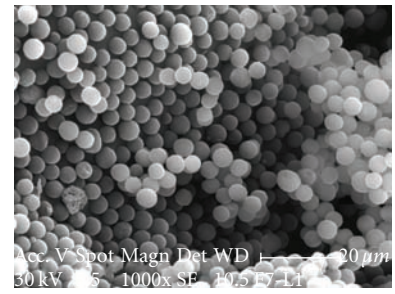

(c)

Figure 3: (a) MPs size distribution as a function of focused and focusing fluid flow rates (▲ 0.25 mL/h–4 mL/min, • ♦ □ 1 mL/h–3 mL/min, ■ 2 mL/min–2 mL/min) (F11) (b) and (c) SEM images examples of particle size distribution.

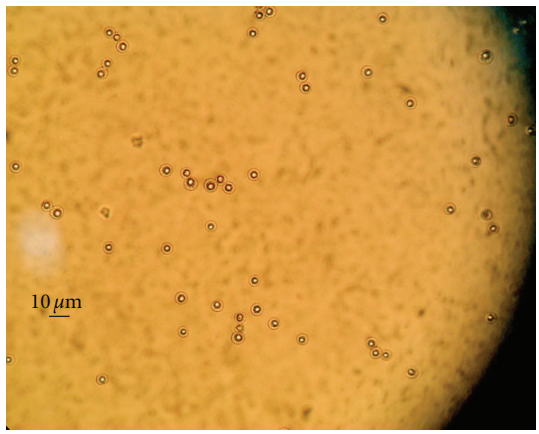

Figure 4: Presence of a dissolution halo for paramagnetic particles elaborated using PSMiso after 10 min incubating in Denhart medium at 90°C.

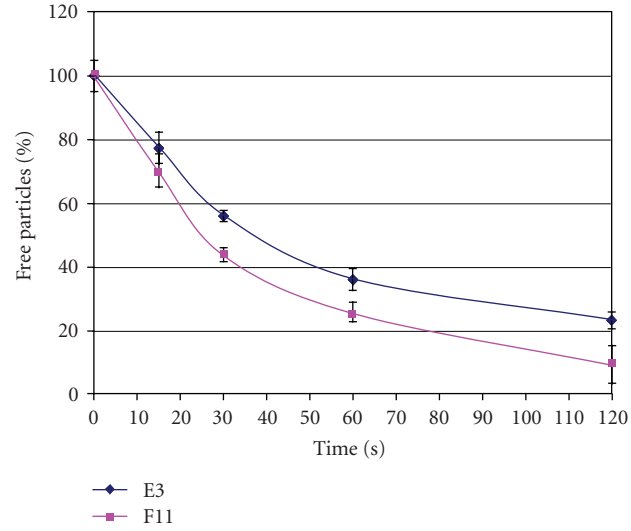

Figure 5: Change in free particles (%) in suspension as a function of magnetic separation time.

Proteins G and A were covalently coupled onto F11-codified microparticle surfaces.

Figure 6(a) shows a fluorescence microscopy image from F11 microparticles codified with rhodamine B.

3.7.1. Analysis of Protein-Protein Interaction. To confirm the union, particles were incubated with a fluorescent-labeled antibody (fluorescein-labeled rabbit antimouse antibody),

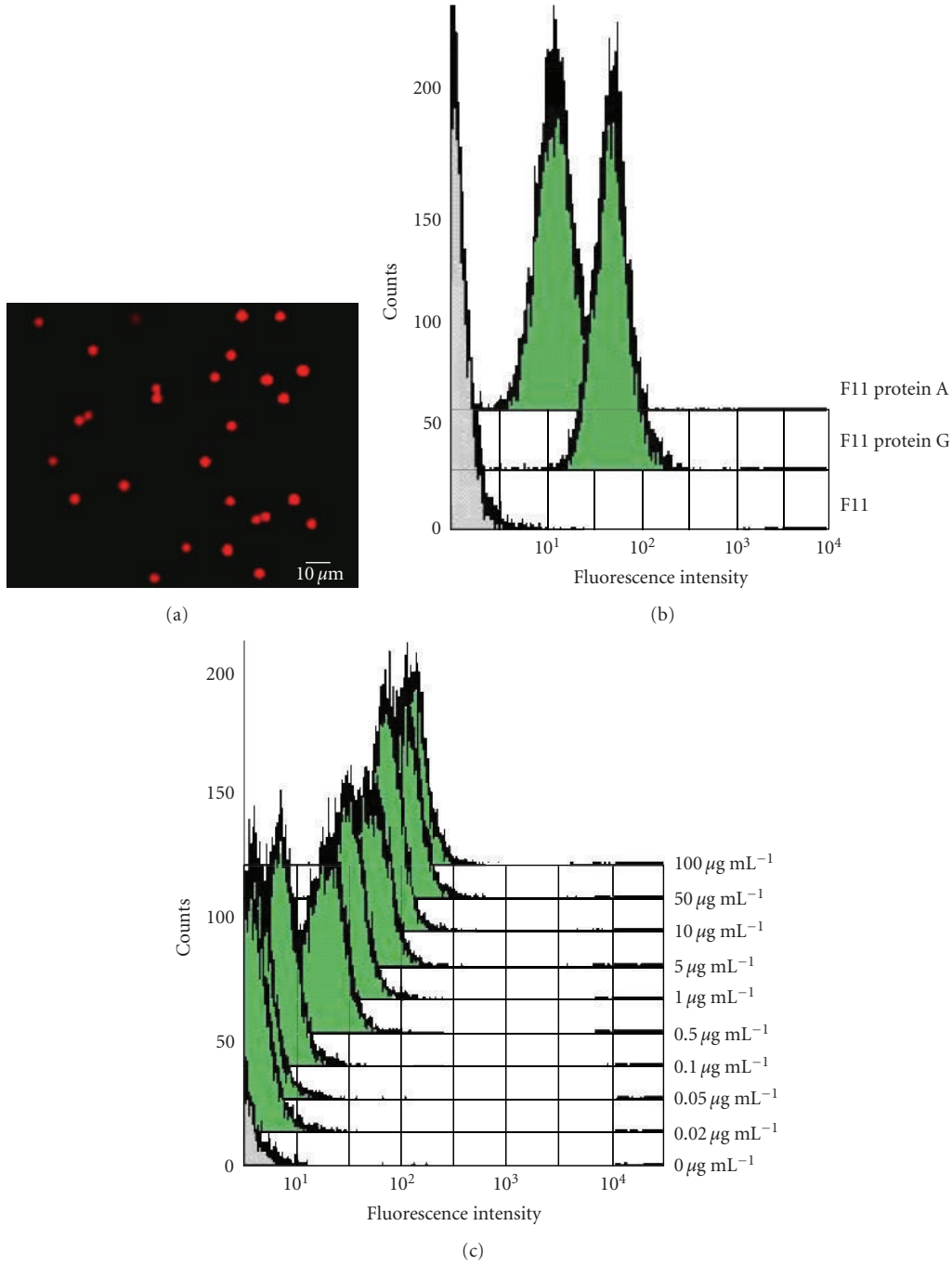

Figure 6: (a) Fluorescence microscope image of paramagnetic microparticles 5 μm in diameter codified with Rhodamine B (formulation F11) and fluorescence flow cytometry profiles for (b) naked E3 microparticles and coupled E3 microparticles with protein G or protein A after incubating with 0.1 mg/ml antibody solution and (c) protein G coupled E3 microparticles after incubation with increasing antibody concentration solutions.

measuring their fluorescence by flow cytometry (FACSCalibur, Becton Dickinson).

0.3 mg of microparticles conjugated to the analyte was incubated for 1 hour in 100 μL of a BSA 1% w/v solution in PBS buffer (pH 7.4). After that, samples were incubated with the fluorescent-labeled antibody in PBS buffer at several concentrations (0–100 μg/mL) for 1 hour, then washed three times with Tween 20 0.02% (v/v), NaCl 2 M, in MES hydrate buffer 50 mM solution, pH 5.4 and then analyzed using flow cytometry.

After coupling protein A or protein G to F11 microparticles and incubating with a 0.1 mg/mL solution of fluorescent-labeled antibody, increased fluorescence was observed in comparison to that from particles not coupled with an

immunoglobulin binding protein (see Figure 6(b)). To confirm that the increased fluorescence was not due to the previously coupled protein, protein G-coupled F11 microparticles were incubated with different fluorescent antibody solutions. An increase in microparticle fluorescence was observed as the concentration of antibody increased (see Figure 6(c)) from 0.02 μg/mL to 50 μg/mL, allowing a quantitative detection for the antibody in this interval of concentrations.

The same experiments were performed with E3 particles (data not shown), and the results were similar.

It is thus possible to conclude that the paramagnetic microparticles produced by FF technology are useful for immunoprecipitation assays.

4. Conclusions

A simple method has been described for the controllable production of functionalized paramagnetic polystyrene microparticles using a combination of flow focusing (FF) and the solvent extraction/evaporation technique. A stable magnetite suspension was produced using silicon oxide as stabilizing agent. Here, a two-phase fluid (magnetite suspension) was flow focused into a laminar capillary microjet to yield monodisperse drops by capillary breakup, showing no differences with a flow-focused single-phase liquid in terms of drop size prediction. This fact confirms the wide range of possible uses of FF, expanding the fluid natures that this technique can accommodate.

The process here reported is potentially a very helpful procedure for efficient microparticle engineering, yielding paramagnetic monodisperse microparticles with diameters of a few microns and a functional surface: a suitable tool for separation processes.

The production of encoded microparticles was also described. The functionality of dye-labelled beads was evaluated allowing conjugation of biomolecules such as proteins. Conjugated microparticles represent a valuable tool for the detection of analyte interactions, using flow cytometry as one of the most accurate and simple techniques for analysis.

To summarize, FF could be regarded as a suitable low-cost alternative for the mass production of high-quality micro-bead arrays and microparticles for separation processes. The dye-labeled microspheres produced have been validated for their useful properties in the analysis of biomolecules.

Notation

C: Polymer concentration (% w/v)
Dg: Drop diameter
Dj: Jet diameter
Dp: Particle diameter
D: Diameter of the outlet orifice (μm)
$D_{0:}$ Inner diameter of the capillary (μm)
D th: Theoretic particle diameter predicted by FF technology (μm)
D_{medium}: Measured mean particle diameter (μm)
EA: Ethyl acetate
EE: Encapsulation efficiency
GSD: Geometrical standard deviation (μm)
H: Distance between the capillary and the outlet (μm)
ICP-MS: Inductively coupled plasma mass spectroscopy
PMDS: Poly(dimethylsiloxane)
PS: Polystyrene
PSMiso: Polystyrene isobutyl
PSMsec: Polystyrene sec-butyl
PVA: Poly(vinyl alcohol)
Qd: Focused fluid flow rate (mL/h)
Qt: Focusing fluid flow rate (mL/minute)
Q: Amount of magnetite encapsulated
Qi: Initial magnetite amount
RhB: Rhodamine B
SEM: Scanning electron microscopy
SD: Standard deviation (μm)
VC: Variation coefficient.

Acknowledgments

This work was funded by the Spanish Ministerio de Ciencia y Tecnología (Project nos. DPI2002-04305-C02-02 and DPI2000-0392-P4-03), Consejería de Innovación de la Junta de Andalucía (Projects nos. 830446 and TEP-1190), and Corporación Tecnológica de Andalucía e Ingeniatrics Tecnologías S.L. L. M.-Banderas, A. R.-Gil and R. G.-Prieto are grateful for financial support from the Spanish Ministerio de Ciencia y Tecnología, University of Sevilla-El Monte Foundation, and Consejería de Innovación de la Junta de Andalucía grants for researcher formation. The numerous suggestions of Dr. A. Cebolla are also gratefully acknowledged.

References

[1] J. Ugelstad, K. H. Kaggerud, F. K. Hansen, and A. Berge, "Absorption of low molecular weight compounds in aqueous dispersions of polymer-oligomer particles. A two step swelling process of polymer particles giving an enormous increase in absorption capacity," *Makromolekulare Chemie*, vol. 180, no. 3, pp. 737–744, 1979.

[2] D. Horák, F. Lednický, E. Petrovský, and A. Kapička, "Magnetic characteristics of ferrimagnetic microspheres prepared by dispersion polymerization," *Macromolecular Materials and Engineering*, vol. 289, no. 4, pp. 341–348, 2004.

[3] J. Wang and S. P. Schwendeman, "Mechanisms of solvent evaporation encapsulation processes: prediction of solvent evaporation rate," *Journal of Pharmaceutical Sciences*, vol. 88, no. 10, pp. 1090–1099, 1998.

[4] D. Tanyolaç and A. R. Özdural, "Preparation of low-cost magnetic nitrocellulose microbeads," *Reactive and Functional Polymers*, vol. 45, no. 3, pp. 235–242, 2000.

[5] S. Omi, A. Kanetaka, Y. Shimamori, A. Supsakulchai, M. Nagai, and G.-H. Ma, "Magnetite microcapsules prepared using a glass membrane and solvent removal," *Journal of Microencapsulation*, vol. 18, no. 6, pp. 749–765, 2001.

[6] R. Wilson, D. G. Spiller, I. A. Prior, K. J. Veltkamp, and A. Hutchinson, "A simple method for preparing spectrally encoded magnetic beads for multiplexed detection," *ACS Nano*, vol. 1, no. 5, pp. 487–493, 2007.

[7] H. Tokoro, T. Nakabayashi, S. Fujii, H. Zhao, and U. O. Häfeli, "Magnetic iron particles with high magnetization useful for immunoassay," *Journal of Magnetism and Magnetic Materials*, vol. 321, no. 10, pp. 1676–1678, 2009.

[8] P. Tartaj, M. del Puerto Morales, S. Veintemillas-Verdaguer, T. González-Carreño, and C. J. Serna, "The preparation of magnetic nanoparticles for applications in biomedicine," *Journal of Physics D*, vol. 36, no. 13, pp. R182–R197, 2003.

[9] M. A. M. Gijs, "Magnetic bead handling on-chip: new opportunities for analytical applications," *Microfluidics and Nanofluidics*, vol. 1, no. 1, pp. 22–40, 2004.

[10] A. K. Gupta and M. Gupta, "Synthesis and surface engineering of iron oxide nanoparticles for biomedical applications," *Biomaterials*, vol. 26, no. 18, pp. 3995–4021, 2005.

[11] S. Rudershausen, C. Grüttner, M. Frank, J. Teller, and F. Westphal, "Multifunctional superparamagnetic nanoparticles for life science applications," *European Cells and Materials*, vol. 3, supplement 2, pp. 81–83, 2002.

[12] N. Wedemeyer, T. Pötter, S. Wetzlich, and W. Göhde, "Flow cytometric quantification of competitive reverse transcription-PCR products," *Clinical Chemistry*, vol. 48, no. 9, pp. 1398–1405, 2002.

[13] S. P. Mulvaney, H. M. Mattoussi, and L. J. Whitman, "Incorporating fluorescent dyes and quantum dots into magnetic microbeads for immunoassays," *Biotechniques*, vol. 36, no. 4, pp. 602–609, 2004.

[14] K. Kriz, F. Ibraimi, M. Lu, L.-O. Hansson, and D. Kriz, "Detection of C-reactive protein utilizing magnetic permeability detection based immunoassays," *Analytical Chemistry*, vol. 77, no. 18, pp. 5920–5924, 2005.

[15] T. Banert and U. A. Peuker, "Synthesis of magnetic beads for bio-separation using the solution method," *Chemical Engineering Communications*, vol. 194, no. 6, pp. 707–719, 2007.

[16] P. Wallemacq, J.-S. Goffinet, S. O'Morchoe et al., "Multi-site analytical evaluation of the abbott ARCHITECT Tacrolimus assay," *Therapeutic Drug Monitoring*, vol. 31, no. 2, pp. 198–204, 2009.

[17] L. Martín-Banderas, M. Flores-Mosquera, A. M. Gañan-Calvo, et al., "Towards high-throughput production of uniformly encoded microparticles," *Advanced Materials*, vol. 18, no. 5, pp. 559–564, 2006.

[18] A. M. Gañán-Calvo, L. Martín-Banderas, R. González-Prieto et al., "Straightforward production of encoded microbeads by Flow Focusing: potential applications for biomolecule detection," *International Journal of Pharmaceutics*, vol. 324, no. 1, pp. 19–26, 2006.

[19] A. M. Gañán-Calvo, "Generation of steady liquid microthreads and micron-sized monodisperse sprays in gas streams," *Physical Review Letters*, vol. 80, no. 2, pp. 285–288, 1998.

[20] R. Bocanegra, J. L. Sampedro, A. Gañán-Calvo, and M. Márquez, "Monodisperse structured multi-vesicle microencapsulation using flow-focusing and controlled disturbance," *Journal of Microencapsulation*, vol. 22, no. 7, pp. 745–759, 2005.

[21] L. Martín-Banderas, M. Flores-Masquera, P. Riesco-Chueca et al., "Flow focusing: a versatile technology to produce size-controlled and specific-morphology microparticles," *Small*, vol. 1, no. 7, pp. 688–692, 2005.

[22] M. A. Holgado, J. L. Arias, M. J. Cózar, J. Álvarez-Fuentes, A. M. Gañán-Calvo, and M. Fernández-Arévalo, "Synthesis of lidocaine-loaded PLGA microparticles by flow focusing. Effects on drug loading and release properties," *International Journal of Pharmaceutics*, vol. 358, no. 1-2, pp. 27–35, 2008.

[23] M. A. Holgado, M. J. Cózar-Bernal, S. Salas, J. L. Arias, J. Álvarez-Fuentes, and M. Fernández-Arévalo, "Protein-loaded PLGA microparticles engineered by flow focusing: physicochemical characterization and protein detection by reversed-phase HPLC," *International Journal of Pharmaceutics*, vol. 380, no. 1-2, pp. 147–154, 2009.

[24] A. M. Gañán-Calvo and P. Riesco-Chueca, "Jetting-dripping transition of a liquid jet in a lower viscosity co-flowing immiscible liquid: the minimum flow rate in flow focusing," *Journal of Fluid Mechanics*, vol. 553, pp. 75–84, 2006.

[25] A. M. Gañán-Calvo and J. M. Gordillo, "Perfectly monodisperse microbubbling by capillary flow focusing," *Physical Review Letters*, vol. 87, no. 27, Article ID 274501, 4 pages, 2001.

[26] A. M. Gañán-Calvo, J. M. Fernández, A. Marquez Oliver, and M. Márquez, "Coarsening of monodisperse wet microfoams," *Applied Physics Letters*, vol. 84, no. 24, pp. 4989–4991, 2004.

[27] S. Takeuchi, P. Garstecki, D. B. Weibel, and G. M. Whitesides, "An axisymmetric flow-focusing microfluidic device," *Advanced Materials*, vol. 17, no. 8, pp. 1067–1072, 2005.

[28] C.-H. Chen, A. R. Abate, D. L. Eugene, E. M. Terentjev, and D. A. Weitz, "Microfluidic assembly of magnetic hydrogel particles with uniformly anisotropic structure," *Advanced Materials*, vol. 21, no. 31, pp. 3201–3204, 2009.

[29] K. P. Yuet, D. K. Hwang, R. Haghgooie, and P. S. Doyle, "Multifunctional superparamagnetic Janus particles," *Langmuir*, vol. 26, no. 6, pp. 4281–4287, 2010.

[30] X. Gong, S. Peng, W. Wen, P. Sheng, and W. Li, "Design and fabrication of magnetically functionalized core/shell microspheres for smart drug delivery," *Advanced Functional Materials*, vol. 19, no. 2, pp. 292–297, 2009.

[31] J. P. Nolan and F. Mandy, "Multiplexed and microparticle-based analyses: quantitative tools for the large-scale analysis of biological systems," *Cytometry A*, vol. 69, no. 5, pp. 318–325, 2006.

[32] K. W. Bong, S. C. Chapin, and P. S. Doyle, "Magnetic barcoded hydrogel microparticles for multiplexed detection," *Langmuir*, vol. 26, no. 11, pp. 8008–8014, 2010.